

Orbital-collapse effects in photoemission from atomic Eu

U. Becker and H. G. Kerkhoff

*Institut für Strahlungs- und Kernphysik, Technische Universität Berlin, D-1000 Berlin 12, West Germany*D. W. Lindle, P. H. Kobrin,* T. A. Ferrett, P. A. Heimann, C. M. Truesdale,[†] and D. A. Shirley*Materials and Molecular Research Division, Lawrence Berkeley Laboratory, University of California,**Berkeley, California 94720**and Department of Chemistry, University of California, Berkeley, California 94720*

(Received 19 May 1986)

Resonant photoelectron spectra of atomic Eu have been measured in the photon-energy ranges of the “ $4d \rightarrow 4f$ ” (110–170 eV) and $3d \rightarrow 4f$ (1120–1165 eV) excitations. For the “ $4d \rightarrow 4f$ ” giant resonance, the decay process results mostly in Eu^+ main-line configurations, including some fractional enhancement directly into the $4d$ continuum. The $3d \rightarrow 4f$ excitations, however, are characterized by competition between the main-line decay channels and channels corresponding to highly excited (satellite) ionic states. We find that decay after $4d$ excitation leads predominantly to the $4f$ continuum, whereas several channels participate in the decay following $3d$ excitation. The observed decay characteristics are discussed with regard to orbital-collapse phenomena.

I. INTRODUCTION

Inner-shell photoabsorption spectra of atomic transition metals exhibit “giant resonances” that have been associated with excitations into partially occupied nd or nf subshells.^{1–4} For the rare-earth metals, these resonances (“ $4d \rightarrow 4f$ ”) have attracted increasing attention in both atomic^{5–8} and solid-state physics.^{9–19} In early work on rare-earth metals,¹ the “ $4d \rightarrow 4f$ ” giant resonances, which generally occur at or slightly above the $4d$ threshold, were ascribed to a multiplet of the discrete $4d \rightarrow 4f$ excitation that is raised into the ϵf continuum by the exchange interaction. Although the description as a discrete resonance raised above its threshold has led to some confusion with regard to giant resonances in atomic systems,²⁰ the association of the resonant intensity with $4d$ excitation to $nf, \epsilon f$ orbitals has been retained.^{2,3,21} In a related development, for atoms just preceding the rare-earth metals in the Periodic Table ($Z \leq 54$), the phenomenon of a delayed onset in the $4d \rightarrow \epsilon f$ continuum has been described as a shape resonance due to the presence of a centrifugal barrier in the effective potential for the excited $4d$ electron.²²

While both giant resonances and shape resonances owe their existence to the presence of a double-well radial potential for the excited or ionized electron, an essential physical difference between these two resonant phenomena is the radial extent of the final-state wave function.^{1,3,4} For the $4d \rightarrow \epsilon f$ shape resonance ($Z \leq 54$), the final state is an uncollapsed continuum ϵf wave function with some resonant localization inside the potential barrier, whereas the “ $4d \rightarrow 4f$ ” giant-resonance state ($Z > 55$) appears more like a discrete state localized in the inner well of the potential.^{3,4}

Recently, a unified approach^{23,24} has related both the “ $4d \rightarrow 4f$ ” resonances (and giant resonances in general) and the $4d \rightarrow \epsilon f$ shape resonances to the orbital-collapse

phenomenon; with increasing atomic number the inner well of the effective potential for an $l=3$ electron deepens rapidly, leading to a decrease in both the energy and size of the $4f$ orbital as it contracts into the inner well over a certain range of Z .^{1–4} In this way, the gradual shift with increasing Z to more and more discrete localized character for the $l=3$ final-state wave function can be described within a single picture.

Considering the orbital-collapse picture, calculations^{23,25} show that the inner well of the effective potential becomes deeper as Z (or the effective charge Z_{eff}) increases, and thus one expects changes in the resonant behavior as a function of Z or Z_{eff} . At low Z (e.g., $Z=36$), no potential barrier exists,²⁵ and the $l=3$ excited-state wave function is governed mostly by the repulsive centrifugal potential. As the Coulombic attraction increases at higher Z (e.g., $Z=54$), an inner well of the potential is formed, and a potential barrier becomes prominent.²² In this range of Z the inner well can support a quasibound state which is trapped by the barrier at a resonance energy; the result is an atomic shape resonance.²⁵ Increasing Z still further (the rare-earth metals), the inner well deepens and the previously quasibound state is pulled lower in energy to near the ionization threshold. In this way, the $l=3$ excited state (not $n=4$, Refs. 2–4) can exist as an eigenstate of both the inner and outer well of the double-well potential,^{3,23} and also can couple to other $l=3$ states that are eigenstates only of the outer well. The excited $l=3$ state for the rare-earth metals can be considered as a hybrid wave function that has appreciable electron density in the vicinity of each well.^{3,4} This resonant hybrid state of both discretelike and continuum-like character results in the so-called “ $4d \rightarrow 4f$ ” giant resonance.^{2–4} Finally, for Z beyond the rare-earth metals, the inner-well becomes deep enough that the $l=3$ eigenstate resides well below the outer well as well as the ionization threshold;^{23,24} no further shape- or giant-resonance

effects can occur.

Experimentally, these effects have been observed in the isonuclear sequence $\text{Ba}, \text{Ba}^+, \text{Ba}^{2+}$, where some resonant components move gradually closer to and finally below the $4d$ threshold with increasing Z_{eff} ,⁷ leading one to conclude that some intermediate hybrid stage between uncollapsed and collapsed wave functions is possible. We expect a similar phenomenon to occur in the same atom if core electrons of different principal quantum numbers (e.g., $3d$ or $4d$) are excited into the $4f$ subshell, because of the accompanying core-hole dependence of Z_{eff} .⁴

The orbital-collapse interpretation of the " $4d \rightarrow 4f$ " giant resonances has its most important implications for the decay characteristics of these resonances. The proposed hybrid character of the final-state wave functions suggests that the " $4d \rightarrow 4f$ " resonances can behave both like a shape resonance by tunneling through the potential barrier and like a discrete (Feshbach) resonance by autoionizing into neighboring continua. These different behaviors can be distinguished experimentally by direct determination of the decay channels of these inner-shell resonances using photoemission. Such an experiment could provide a very sensitive probe of the effective potential for $l=3$ electrons in the rare-earth metals. In this paper we report the first such measurements for atomic " $4d \rightarrow 4f$ " and $3d \rightarrow 4f$ excitations, which we have studied in atomic Eu, an element for which the oscillator strength of the " $4d \rightarrow 4f$ " excitation peaks above the $4d_{5/2}$ ionization threshold. The " $4d \rightarrow 4f$ " data yield comprehensive results on the relative contributions of discrete autoionization and continuum shape-resonance decay channels to deexcitation of atomic giant resonances. In contrast, the $3d \rightarrow 4f$ excitations are discrete transitions to the partially filled $4f$ subshell, and therefore lie below their respective $3d$ ionization limits. The direct comparison of decay characteristics for these qualitatively different inner-shell resonances in Eu can provide a sensitive test of the orbital-collapse description of giant resonances.

The experiment is described briefly in Sec. II, followed in Sec. III by a discussion of the results. Conclusions appear in Sec. IV.

II. EXPERIMENTAL

The measurements were made at the Stanford Synchrotron Radiation Laboratory (SSRL) using a time-of-flight (TOF) electron spectrometer described elsewhere.²⁶ The Eu vapor was introduced into the spectrometer with a resistively heated oven that has been used in previous photoemission experiments.²⁷ Photons in the energy ranges of the $4d$ and $3d$ excitations were obtained from SSRL Beam Lines III-1 (grasshopper monochromator) and III-3 (JUMBO), respectively. Calibration of the photon energy to within 1 eV was accomplished by comparison with known photoabsorption data⁵ for the " $4d \rightarrow 4f$ " resonance measurements, and by measuring a $\text{Ne } 1s \rightarrow 3p$ (867-eV photon energy) excitation spectrum for the $3d \rightarrow 4f$ measurements. The energy levels in Eu relevant to this work are depicted in Fig. 1.

Monitoring the photoemission intensity at 54.7° relative to the photon polarization vector provided the relative

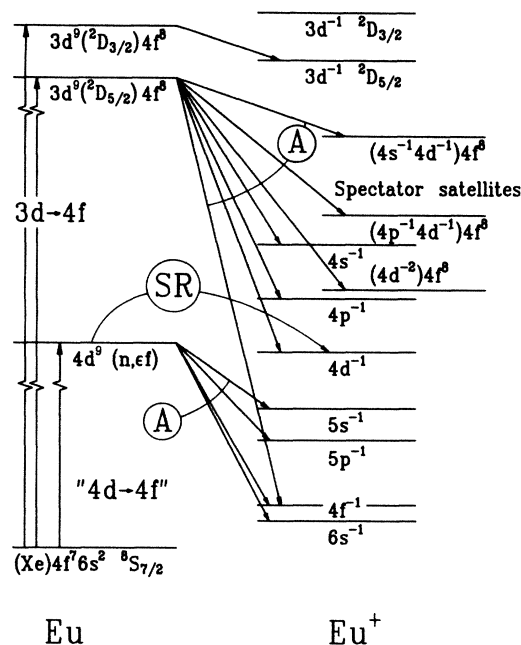


FIG. 1. Energy-level diagram of Eu, indicating the transitions studied. A is autoionization, SR is shape resonance. The " $4d \rightarrow 4f$ " multiplet structure, which has little importance to the resonant decay characteristics, is neglected here. Some decay channels have been omitted for clarity.

total-yield spectra shown in Fig. 2 taken in the photon-energy ranges of the Eu " $4d \rightarrow 4f$ " and $3d \rightarrow 4f$ excitations. Figure 3 shows photoelectron TOF spectra taken at selected photon energies. The TOF spectra in Fig. 3(a) were both taken at $h\nu=138$ eV, on the low-energy side of the " $4d \rightarrow 4f$ " resonance, which peaks at $h\nu=141$ eV be-

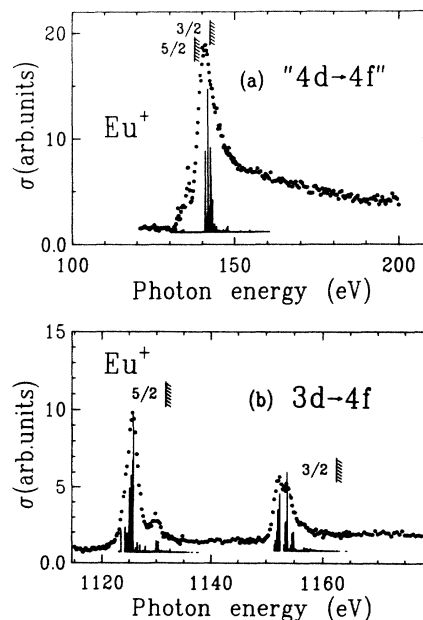


FIG. 2. Total-yield spectra of Eu in the photon-energy ranges of the (a) " $4d \rightarrow 4f$ " and (b) $3d \rightarrow 4f$ resonances. Solid lines represent calculations of the multiplet structure as described in the text.

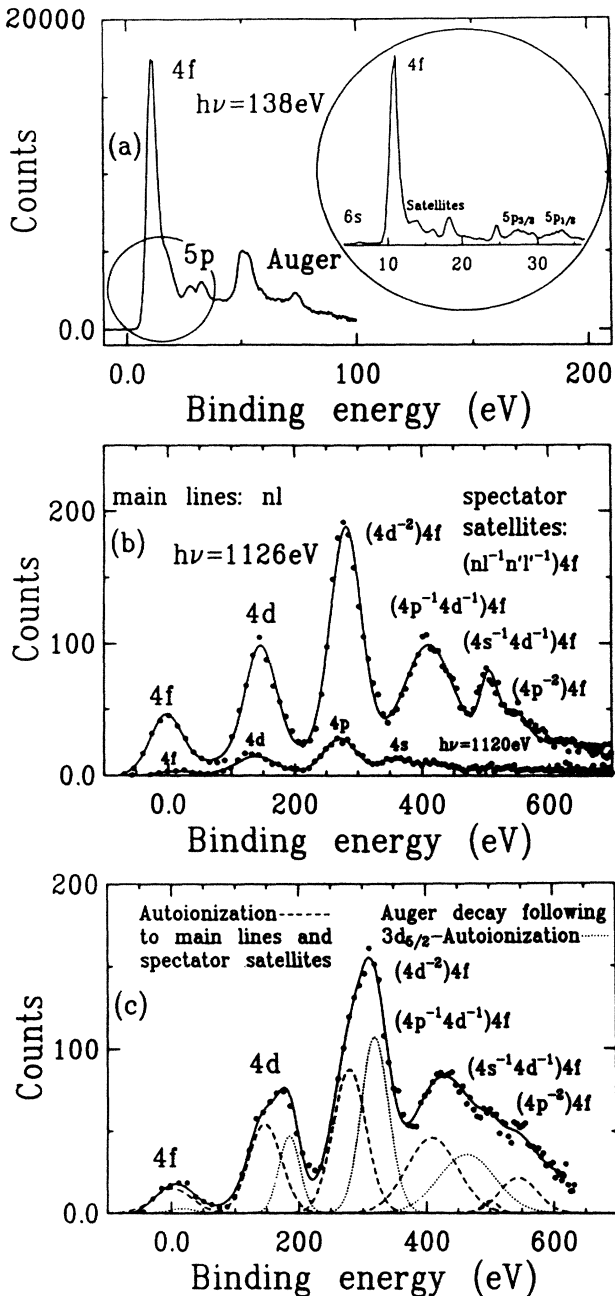


FIG. 3. TOF photoelectron spectra of Eu taken with photon energies of (a) 138 eV near the “ $4d \rightarrow 4f$ ” resonance, (b) 1126 eV at the maximum of the $3d_{5/2}$ spin-orbit component of the $3d \rightarrow 4f$ resonance, compared to a nonresonant spectrum at $h\nu = 1120$ eV [lower part of (b)], and (c) 1153 eV at the maximum of the $3d_{3/2}$ component of the $3d \rightarrow 4f$ resonance. The Auger peaks in (a) result from decay of $\text{Eu}^+ 4d^{-1}$ hole states. The inset in (a) shows the presence of spin-flip satellites of the $4f$ peak, whose intensities mimic the $4f$ main-line cross section. The peak assignments in (b) and (c) are discussed in the text and refer to the ionized electron (e.g., $4f$) or to the final-ionic-state configuration (e.g., $4d^{-2}4f$). In (c) the photon energy exceeds the $3d_{5/2}$ threshold, and thus we observe Auger decay from this Eu^+ state. The dashed and dotted curves in (c) represent autoionization electrons from the decay of $\text{Eu}^*(3d_{3/2}4f)$ and Auger electrons from the decay of $\text{Eu}^+(3d_{5/2})$, respectively.

tween the $4d_{5/2}$ and $4d_{3/2}$ thresholds. The TOF spectra in Fig. 3(b) were taken at $h\nu = 1126$ eV right on the peak of the $3d_{5/2} \rightarrow 4f$ resonance (top), and off-resonance at $h\nu = 1120$ eV (bottom). Finally, in Fig. 3(c) we show a TOF spectrum at $h\nu = 1153$ eV, on the $3d_{3/2} \rightarrow 4f$ resonance. The $4d_{5/2,3/2}$ and $3d_{5/2,3/2}$ thresholds (137.5, 142.6, 1131, and 1163 eV, respectively) shown in Fig. 2 were derived from $4d$ and $3d$ photoelectron kinetic energies measured at photon energies above each threshold.

III. RESULTS AND DISCUSSION

The total-yield measurements in Fig. 2 are equivalent to photoabsorption spectra for the “ $4d \rightarrow 4f$ ” and $3d \rightarrow 4f$ resonance regions. In Fig. 2 we compare the experimental results with multiplet-structure calculations of the allowed discrete transitions for both resonances. The calculations were performed using a program of Cowan,²⁸ and the energy positions were adjusted to coincide with experimental values. Our results for $3d \rightarrow 4f$ excitation are in good agreement with similar calculations by Thole *et al.*²⁹

The calculations show very good agreement with the $3d \rightarrow 4f$ total-yield spectrum, as one would expect for purely discrete transitions. However, agreement with the “ $4d \rightarrow 4f$ ” data is not as good. Neither the asymmetric shape nor the extraordinary width of the giant resonance is predicted by the calculations, indicating some significant qualitative difference between the $l = 3$ wave functions reached by excitation from the $3d$ or $4d$ orbitals. As we discuss below, distinctions between the $3d \rightarrow 4f$ and “ $4d \rightarrow 4f$ ” excitations will become even more clear when we consider the resonant decay characteristics as studied by photoemission.

Moving on to the photoelectron-spectroscopy results, Sec. III A will first present a description of the available final-ionic-state channels for the decay of the “ $4d \rightarrow 4f$ ” and $3d \rightarrow 4f$ resonances in terms of decay modes. Using the decay modes defined in Sec. III A, we then discuss in Sec. III B the photoemission results in the $4d$ and $3d$ energy ranges.

A. Resonant decay channels

Many photoemission decay channels are allowed following the $3d \rightarrow 4f$ and “ $4d \rightarrow 4f$ ” excitations. For discussion of the “ $4d \rightarrow 4f$ ” resonance results, we shall group the decay channels into two principal decay modes.

(1) In decay mode 1, the “ $4d \rightarrow 4f$ ” excited state may resemble a shape resonance. In this decay mode, the $4d$ electron experiences a continuum enhancement near threshold that is related to the presence of a potential barrier for the excited electron. The result is a (main line) $\text{Eu}^+ 4d^{-1}$ photoemission final state. Connerade³⁰ has discussed this channel in the context of a shape-independent model.³¹

(2) In decay mode 2, the “ $4d \rightarrow 4f$ ” excited state may resemble an autoionization resonance. In this decay mode, the excited $4d$ electron experiences significant interchannel coupling to many continua. The result is photoemission producing Eu^+ configurations correspond-

ing to main lines other than $4d^{-1}$, and their correlation and spin-flip satellites.

It should be recognized that these simplified descriptions of decay modes are limited by our incomplete understanding of the decay dynamics of giant resonances, but they are useful in describing the observed decay character of the giant resonance. As discussed in Sec. I, the relative importance of decay modes 1 and 2 to deexcitation of a giant resonance may signify in some way the effects of orbital collapse on the resonant decay process.

For the discrete $3d \rightarrow 4f$ resonances, decay mode 1 described above would lead to $3d_{5/2}$ or $3d_{3/2}$ photoemission, but is energetically inaccessible for each spin-orbit component. The remaining decay mode via $3d \rightarrow 4f$ autoionization (decay mode 2) therefore encompasses all possible Eu^+ photoemission final states. For discussion of the $3d \rightarrow 4f$ resonances, we divide decay mode 2 according to the "spectator" character of the excited $4f$ electron, as follows.

(a) The $4f$ subshell to which the $3d$ electron was excited is involved in the decay, resulting in Eu^+ main-line (single-hole) configurations.³²

(b) The $4f$ subshell, including the excited $4f$ electron, remains as a spectator to the decay process, resulting in satellite (double-hole plus excited electron) configurations of Eu^+ containing eight $4f$ electrons. We shall refer to these configurations as spectator satellites.³³

The differentiation of decay modes 2 (a) and (b) is possible in the case of the $3d \rightarrow 4f$ resonances because the $3d$ excitation process populates the *discrete* $4f$ orbital. In contrast, the $4d$ electron excited in the case of the " $4d \rightarrow 4f$ " resonance is placed in a *hybrid* $l=3$ state, that is not simply described as $n=4$.²⁴ In fact, this hybrid state reached in the " $4d \rightarrow 4f$ " excitation has been described²⁻⁴ as similar to a discrete $5f$ wave function inside the potential barrier (i.e., at low atomic radial distance r), and similar to a continuum ϵf wave function outside the potential barrier (at high r). This hybrid character can be considered a direct consequence of the orbital-collapse phenomenon moderated by the potential barrier for the excited electron.

B. Photoemission results

In the " $4d \rightarrow 4f$ " resonance case, the photoelectron spectra in Fig. 3(a) qualitatively illustrate the dominance of decay mode 2 over production of $\text{Eu}^+ 4d^{-1}$ (represented in the spectra by Auger electrons following $4d$ photoemission) via decay mode 1. Furthermore, we also observe that autoionization to the $4f^{-1}$ final state is the dominant decay channel within decay mode 2. The favored deexcitation channel for the giant resonance is thus the super-Coster-Kronig-like decay $4d^9 4f^7(4, \epsilon f) \rightarrow 4d^{10} 4f^6(\epsilon d, g)$, leaving the ion in the same final state as reached by direct $4f$ photoemission.^{34,35} Figure 4 shows the partial cross sections for $4d$, $4f$, $5p$, and $6s$ photoemission in the vicinity of the " $4d \rightarrow 4f$ "

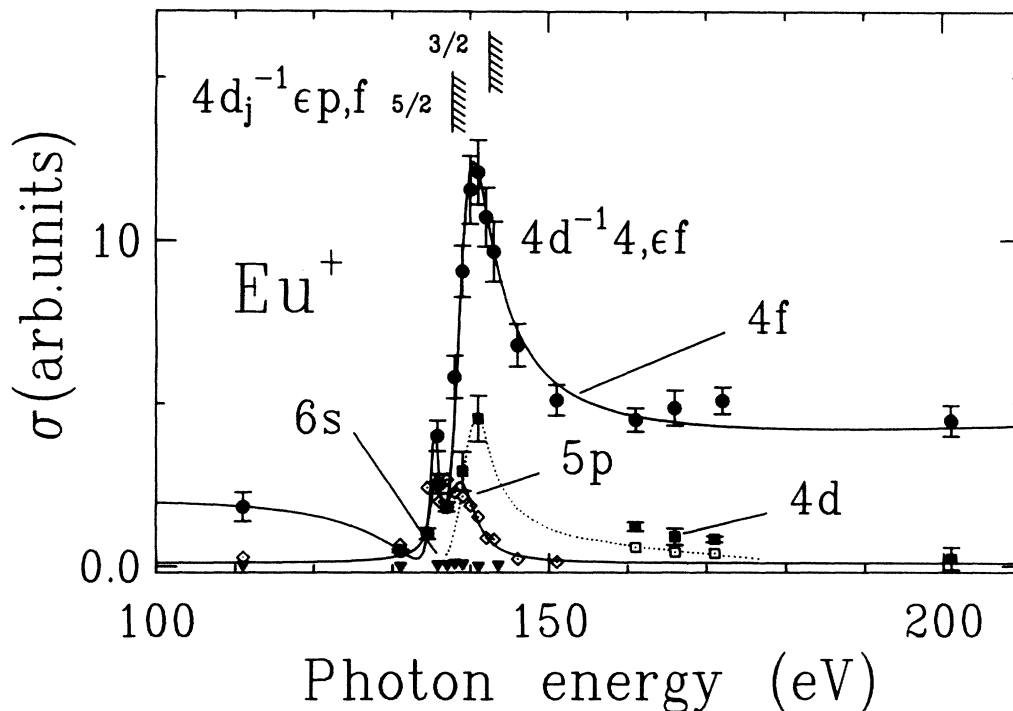


FIG. 4. Partial cross sections of the $4d$ (squares, open squares for $4d_{5/2}$ only), $4f$ (circles), $5p$ (diamonds), and $6s$ (triangles) main lines in the vicinity of the " $4d \rightarrow 4f$ " giant resonance. The solid curves represent two-resonance fits with Beutler-Fano profiles. The dotted line represents the $4d_{5/2}$ cross section in the shape-independent approximation (Refs. 19 and 30).

resonance, quantitatively confirming these conclusions. A similar result for the $4f$ cross section was obtained from the corresponding constant-initial-state spectrum of Eu metal.¹⁶

The $4d$ photoemission cross section measured above 160 eV accounts for less than 25% of the total photoabsorption cross section. Auger electrons from decay of $4d$ -hole states were observed at lower photon energies near the peak of the giant resonance, and were used to determine the $4d$ cross-section near threshold. The data in Fig. 4 show explicitly that photoemission into the $4d$ continuum (decay mode 1) is less likely than decay into the $4f$ continuum (decay mode 2), confirming a calculation by Amusia *et al.*³⁶ The results in Fig. 4 also suggest that it is useful to picture the $l=3$ orbital reached by the giant-resonance excitation as a wave function in which discrete-like and continuumlike components couple to different decay channels (decay modes 2 and 1, respectively). In some sense, the relative contributions of the discrete and continuum decay-modes determine the degree of orbital collapse of the excited wave function. In the case of Eu " $4d \rightarrow 4f$ ", which has considerable discrete decay character (decay mode 2), it may be appropriate to consider the excited state as mostly, but not completely, collapsed. Finally, the importance of both decay modes 1 and 2 for the " $4d \rightarrow 4f$ " resonance demonstrates that photoabsorption spectra of giant resonances are insufficient to test either calculations based on discrete transitions alone,²⁸ or the shape-independent approximation of the continuum resonance;^{19,30} measurements of partial cross sections are required.

Turning to the $3d \rightarrow 4f$ excitations, the spectra in Fig. 3(b) below the $3d_{5/2}$ threshold show that several main-line and spectator-satellite channels are enhanced on resonance. As mentioned in Sec. I, the removal of a $3d$ electron causes a large enough increase in Z_{eff} so that the $3d_{5/2,3/2} \rightarrow 4f$ excitations are discrete, in contrast to the " $4d \rightarrow 4f$ " resonance.

Comparing peaks in the resonant and nonresonant spectra in Fig. 3(b) to estimated binding energies and intensities (the former estimated as differences of one-electron neutral binding energies for the appropriate subshells, and the latter determined by reference to calculated Auger intensities³⁷), we propose the following assignments of the photoemission peaks in the *resonant* spectrum only. The first two peaks should correspond primarily to autoionization to the $4f$ and $4d$ mainlines, respectively. The third peak contains the $4d^{-2}4f^8$ spectator satellite and the $4p$ main line, although the intensity estimates suggest that the $4d^{-2}4f^8$ satellite will be largest. Based on binding energies alone, the last two prominent features most likely are due to spectator transitions to the $4p^{-1}4d^{-1}4f^8$ and $4s^{-1}4d^{-1}4f^8$ configurations, respectively. The peaks in the nonresonant spectrum at $h\nu=1120$ eV almost certainly correspond just to main-line Eu^+ configurations, because the (highly excited) spectator-satellite cross sections will be extremely small off resonance. The limited resolution of the TOF spectra is insufficient to measure the absolute quantitative relationship between autoionization into the main-line [decay mode 2(a)] and spectator [decay mode 2(b)] channels, but it does show qualitatively the competition between the two modes.

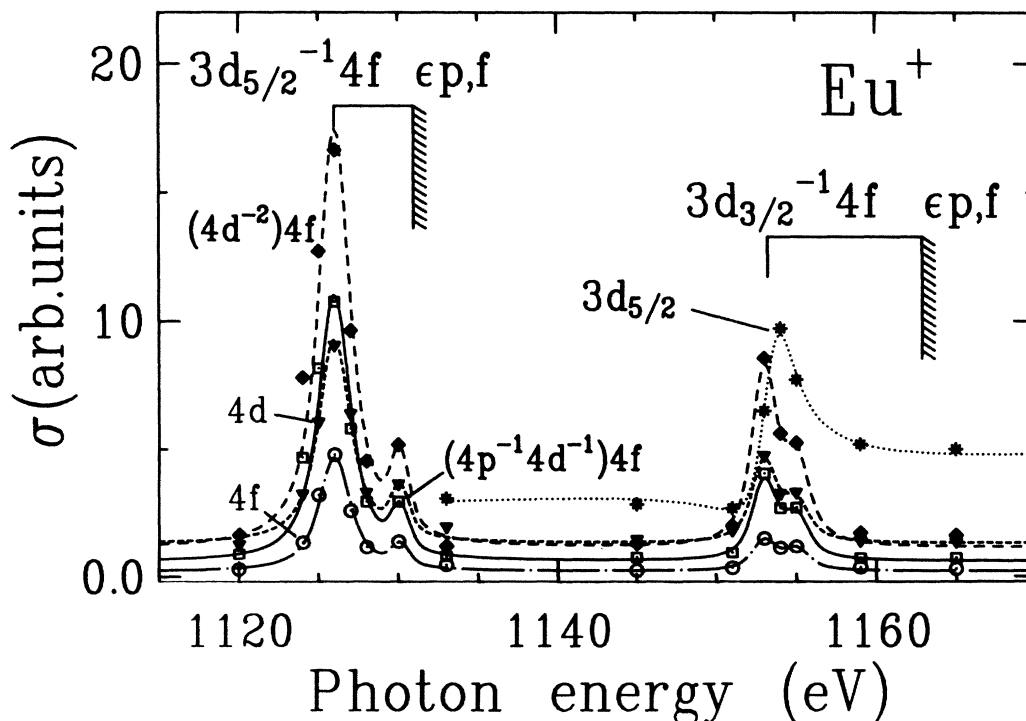


FIG. 5. Partial cross sections of the $4d$ (triangles), $4f$ (circles), and $3d_{5/2}$ (stars) main lines, and the $4d^{-2}4f^8$ (diamonds) and $4p^{-1}4d^{-1}4f^8$ (squares) satellites in the $3d \rightarrow 4f$ excitation region.

For the $3d_{3/2} \rightarrow 4f$ excitation, the $3d_{5/2}$ main-line state also can be reached by autoionization, and in fact this channel accounts for almost half of the total intensity at the $3d_{3/2} \rightarrow 4f$ resonance [see Fig. 3(c)]. This result is in good agreement with theoretical predictions for La,³⁸ and is consistent with the asymmetric line shape of the $3d_{3/2}$ resonance in our total-yield spectrum, which arises from interference between the direct and resonant ionization contributions. We conclude that autoionization to the main $n=3,4$ photoemission final states contributes considerably to the decay of the $3d \rightarrow 4f$ excitations, especially for the $3d_{3/2}$ spin-orbit component.

In Fig. 5 we show the relative intensities of the photoemission peaks that primarily correspond to the $4d$, $4f$, and $3d_{5/2}$ main-line channels and the $4d^{-2}4f^8$ and $4p^{-1}4d^{-1}4f^8$ spectator satellites (the “ $4f$ peak” includes contributions from the $5s$, $5p$, and $6s$ subshells, and the satellites include some $4p$ and $4s$ main-line intensity, respectively) in the $3d \rightarrow 4f$ excitation energy range. Above the $3d_{3/2}$ threshold, Auger electrons from the decay of $3d_{5/2}$ hole states are unresolved from the main-line and spectator-satellite photoemission peaks, as can be seen in Fig. 3(c). Therefore, the measurements in Fig. 5 above 1131-eV photon energy should be considered as qualitative results only.

The results in Fig. 5 show that there is no favored decay channel following $3d \rightarrow 4f$ excitation, in contrast to the “ $4d \rightarrow 4f$ ” resonance, but rather that many continua participate in the decay of the excited states. Enhancement of the satellites shows that autoionization via spectator transitions [decay mode 2(b)] is competitive in the decay of a $3d$ hole state. The competition between main-line [decay mode 2(a)] and satellite [decay mode 2(b)] Eu^+ final states can be viewed as a result of the more compact size of the collapsed wave function for the excited $4f$ electron. By virtue of being strongly localized in the inner well of the potential, the excited resonant state couples significantly with many continua, producing autoionization to both main-line and spectator satellite channels. Finally, our observations of decay to the $4f^{-1}$ state corroborate findings by inverse photoemission¹⁰ as well as by direct valence-band photoemission obtained recently for different rare-earth-metal compounds.¹⁸

IV. CONCLUSIONS

In conclusion we have observed that autoionization to main-line final states (mostly $4f^{-1}$) is the dominant decay mode for the “ $4d \rightarrow 4f$ ” giant resonance in Eu, although this resonance exhibits some “shape-resonance character” as well. The decay of the $3d \rightarrow 4f$ resonances shows competition between autoionization to main-lines and spectator-satellites. The populations of the different decay channels change dramatically with the quantum number of the core hole created. This quantitative difference in decay-channel cross sections is probably related to the core-level-vacancy dependence of the excited-state potential and thereby the orbital-collapse phenomenon, which can modify the $l=3$ excited-state wave function. The collapsed $4f$ wave function following $3d \rightarrow 4f$ excitation produces a strong discrete autoionizing resonance by virtue of being completely localized in the inner well of the atomic potential, whereas the $l=3$ wave function populated by the “ $4d \rightarrow 4f$ ” excitation may be regarded as a hybrid inner-well eigenstate with some continuum character that produces both autoionizationlike (decay mode 2) and shape-resonance-like decay (decay mode 1). A complete understanding of how these differing intermediate-state wave functions affect the different decay-channel probabilities will require further theoretical analysis and experimental studies. Finally, we expect that the decay characteristics observed in Eu also will be found in other rare-earth metals.

ACKNOWLEDGMENTS

This work was supported by the Director, Office of Energy Research, Office of Basic Energy Sciences, Chemical Sciences Division of the U.S. Department of Energy under Contract No. DE-AC03-76SF00098. It was performed at the Stanford Synchrotron Radiation Laboratory, which is supported by the Department of Energy's Office of Basic Energy Sciences. One of us (U.B.) acknowledges funding by the Bundesministerium für Forschung und Technologie (BMFT) and another (H.G.K.) support by the Wigner Foundation.

*Present address: Rockwell International, P.O. Box 1085, Thousand Oaks, CA 91360.

†Present address: Research and Development Division, Corning Glass Works, Corning, NY 14831.

¹J. L. Dehmer, A. F. Starace, U. Fano, J. Sugar, and J. W. Cooper, *Phys. Rev. Lett.* **26**, 1521 (1971).

²G. Wendin, *J. Phys. B* **9**, L297 (1976); G. Wendin and A. F. Starace, *ibid.* **11**, 4119 (1978).

³J. P. Connerade, *Contemp. Phys.* **19**, 415 (1978).

⁴R. I. Karaziya, *Usp. Fiz. Nauk* **135**, 79 (1981) [*Sov. Phys.—Usp.* **24**, 775 (1981)].

⁵M. W. D. Mansfield and J. P. Connerade, *Proc. R. Soc. London Ser. A* **352**, 125 (1976).

⁶E. -R. Radtke, *J. Phys. B* **12**, L71 (1979); **12**, L77 (1979).

⁷T. B. Lucatorto, T. J. McIlrath, J. Sugar, and S. M. Younger,

Phys. Rev. Lett. **47**, 1124 (1981).

⁸R. C. Karnatak, J. M. Esteve, and J. P. Connerade, *J. Phys. B* **14**, 4747 (1981).

⁹T. M. Zimkina, V. A. Fomichev, S. A. Gribovskii, and I. I. Zhukova, *Fiz. Tverd. Tela. (Leningrad)* **9**, 1447 (1967) [*Sov. Phys.—Solid State* **9**, 1128 (1967)].

¹⁰M. B. Chamberlain, A. F. Burr, and R. J. Liefeld, *Phys. Rev. A* **9**, 663 (1974).

¹¹C. Bonelle, R. C. Karnatak, and N. Spector, *J. Phys. B* **10**, 795 (1977).

¹²W. Lenth, F. Lutz, J. Barth, G. Kalkoffen, and C. Kunz, *Phys. Rev. Lett.* **41**, 1185 (1978).

¹³J. W. Allen, L. I. Johansson, R. S. Bauer, I. Lindau, and S. B. M. Hagstrom, *Phys. Rev. Lett.* **41**, 1499 (1978).

¹⁴W. F. Egelhoff, G. G. Tibbets, M. H. Hecht, and I. Lindau,

- Phys. Rev. Lett. **46**, 1071 (1981).
- ¹⁵M. H. Hecht and I. Lindau, Phys. Rev. Lett. **47**, 821 (1981).
- ¹⁶F. Gerken, J. Barth, and C. Kunz, Phys. Rev. Lett. **47**, 993 (1981); *Proceedings of the International Conference on X-Ray and Atomic Inner-Shell Physics, Eugene, Oregon, 1982*, AIP Conf. Proc. No. 94, edited by B. Crasemann (AIP, New York, 1982).
- ¹⁷G. Kaindl, G. Kalkowski, W. D. Brewer, B. Perscheid, and F. Holtzberg, J. Appl. Phys. **55**, 1910 (1984).
- ¹⁸J. W. Allen, S. J. Oh, I. Lindau, and L. I. Johansson, Phys. Rev. B **29**, 5927 (1984).
- ¹⁹J. P. Connerade and M. Pantelouris, J. Phys. B **17**, L173 (1984).
- ²⁰J. P. Connerade and M. W. D. Mansfield, Proc. R. Soc. London Ser. A **341**, 267 (1974); D. L. Ederer, T. B. Lucatorto, E. B. Saloman, R. P. Madden, and J. Sugar, J. Phys. B. **8**, L21 (1975).
- ²¹J. E. Hansen, A. W. Fliflet, and H. P. Kelly, J. Phys. B **8**, L127 (1975).
- ²²M. Goepfert-Mayer, Phys. Rev. **60**, 184 (1941); J. W. Cooper, Phys. Rev. Lett. **13**, 762 (1964).
- ²³K. T. Cheng and C. Froese-Fischer, Phys. Rev. A **28**, 2811 (1983).
- ²⁴K. T. Cheng and W. R. Johnson, Phys. Rev. A **28**, 2820 (1983).
- ²⁵S. T. Manson and J. W. Cooper, Phys. Rev. **165**, 126 (1968).
- ²⁶M. G. White, R. A. Rosenberg, G. Gabor, E. D. Poliakoff, G. Thornton, S. Southworth, and D. A. Shirley, Rev. Sci. Instrum. **50**, 1288 (1979).
- ²⁷P. H. Kobrin, U. Becker, S. Southworth, C. M. Truesdale, D. W. Lindle, and D. A. Shirley, Phys. Rev. A **26**, 842 (1982).
- ²⁸R. Cowan, J. Opt. Soc. Am. **58**, 808 (1968); *The Theory of Atomic Structure and Spectra* (University of California Press, Berkeley, 1981).
- ²⁹B. T. Thole, G. van der Laan, J. C. Fuggle, G. A. Sawatzky, R. C. Karnatak, and J. E. Esteva (unpublished).
- ³⁰J. P. Connerade, J. Phys. B **17**, L165 (1984); see also J. R. Peterson, Y. K. Bae, and D. L. Huestis, Phys. Rev. Lett. **55**, 692 (1985).
- ³¹The shape-independent model (Ref. 30) treats giant resonances as shape-resonance phenomena which arise from strong overlap between the inner-well excited state and high- l continuum final states at a well-defined energy (Ref. 25), yielding a formula that predicts a resonance shape different than a Beutler-Fano profile. Such an interpretation regards continuum giant resonances as an effect within a single channel, in contrast to autoionization which is an interchannel effect.
- ³²Because of the difference in spins of the electron excited to the $4f$ orbital and the "other" seven $4f$ electrons, the term symbols for the Eu^+ main-line configurations produced will vary. However, the present low-resolution results only distinguish among the different configurations.
- ³³Other satellites that do not have an extra $4f$ electron are possible but do not have this spectator character, and therefore are included implicitly in decay mode 2(a).
- ³⁴E. J. McGuire, J. Phys. Chem. Solids **33**, 577 (1972).
- ³⁵In a different model, decay of the " $4d \rightarrow 4f$ " resonance is described by collective oscillations. See A. Zangwill and P. Soven, Phys. Rev. Lett. **45**, 204 (1980).
- ³⁶M. Y. Amusia, S. I. Sheftel, and L. V. Chernysheva, Zh. Tekh. Fiz. **51**, 2441 (1981) [Sov. Phys.—Tech. Phys. **26**, 1444 (1981)].
- ³⁷E. J. McGuire, Phys. Rev. A **5**, 1052 (1972).
- ³⁸F. Combet Farnoux, Phys. Rev. A **25**, 287 (1982); *Abstracts of Contributed Papers, Thirteenth International Conference on the Physics of Electronic and Atomic Collisions, Berlin, 1983*, edited by J. Eichler, W. Fritsch, I. V. Hertel, N. Stotterfoht, and U. Wille (ICPEAC, Berlin, 1983); see also G. Wendin, Phys. Rev. Lett. **53**, 724 (1984).